# Investigation of the $^{3}\mathrm{He}\,\eta$ final state in the $\vec{d}p \to {}^{3}\mathrm{He}\,\eta$ reaction at ANKE


A. Khoukaz, T. Mersmann, M. Mielke, M. Papenbrock,
T. Rausmann, J.P. Wessels
*Institut für Kernphysik, Universität Münster*
*Wilhelm-Klemm-Str. 9, D-48149 Münster, Germany*

D. Chiladze, V. Hejny, I. Keshelashvili, F. Rathmann, H. Ströher
*Institut für Kernphysik, Forschungszentrum Jülich,*
*D-52425 Jülich, Germany*

A. Kacharava
*Physikalisches Institut II, Universität Erlangen-Nürnberg,*
*D-91058 Erlangen, Germany*

B. Chiladze, N. Lomidze, M. Nioradze
*High Energy Physics Institute, Tbilisi State University,*
*0186 Tbilisi, Georgia*

D. Dymov, D. Gusev, A. Kulikov, V. Kurbatov,
G. Macharashvili, Yu. Uzikov
*Joint Institute for Nuclear Research, LNP,*
*141980 Dubna, Russia*

C. Hanhart, A. Sibirtsev
*Institut für Theoretische Physik, Forschungszentrum Jülich,*
*D-52425 Jülich, Germany*

A. Wrońska
*Institute of Nuclear Physics,*
*31342 Cracow, Poland*

C. Wilkin
*University College London, London, WC1E 6BT, UK*

and the ANKE collaboration

Spokesperson: T. Rausmann (`trausmann@uni-muenster.de`)


April 5, 2006

**Abstract**

Measurements of the near–threshold production of the $^3\mathrm{He}\,\eta$ final state in deuteron-proton collisions are of great interest. There are still many open questions concerning the $\eta$–nucleon force, the $\eta$–nucleus final–state interaction (FSI) and threshold enhancement, and the possible existence of quasi–bound $\eta$–nucleus states. Very successful measurements have recently been carried out at ANKE, which will lead to very high precision data on total and differential cross sections both in the vicinity of the threshold as well as at intermediate excess energies up to $Q = 60\,\mathrm{MeV}$. The very low statistical errors required for the precise determination of the real and imaginary parts of the $\eta^3\mathrm{He}$ scattering length have been achieved using an unpolarized beam and target.

However, if the FSI interpretation is correct, the effect of the strong enhancement in the total cross section close to the production threshold should depend only weakly upon the characteristics of the entrance channel and it is very important to verify this. We therefore apply for two weeks of beam time to investigate the spin dependence of the near–threshold behaviour of the excitation function of the reaction $\vec{d}p \to {}^3\mathrm{He}\,\eta$ using a polarized COSY deuteron beam. At a later stage it is planned to extend these studies by measurements at ANKE with a polarized target in addition to a polarized beam.

# 1 Introduction

For more than a decade the $\eta$ interaction with nucleons and nuclei has attracted much attention both experimentally and theoretically. One reason for this excitement is the possibility of the formation of $\eta$–nucleus bound states. The existence of so–called $\eta$–mesic nuclei was first predicted by Haider and Liu [1], based on the observation that the elementary $\eta N$ interaction is attractive and relatively strong [2]. It is expected that the attraction gets stronger with increasing nuclear mass number and eventually should lead to a bound state. However, it is so far unclear for which mass number that might actually happen. For example, in the literature one can find speculations that even the $\eta d$ system might form such a bound state [3], though this is disputed by other investigators [4]. More conservative workers consider the $\eta^4\mathrm{He}$ system as the lightest possible candidate [5, 6, 7]. Heavier nuclei were studied theoretically, *e.g.* in Ref. [8], where it was concluded that, although there should be bound states, their width could be of the order of the binding energy, making direct observations of these states very difficult. Experimentally a first indication for the possible existence of a $\eta^3\mathrm{He}$ bound state was reported in photoproduction in Ref. [9], though this interpretation is not without ambiguity [10].

The occurrence of a bound state near the reaction threshold will also be reflected in the corresponding $\eta$–nucleus scattering length $a$ [11]. In such a case the real part of the scattering length should be relatively large and negative whereas its imaginary part should be small. Studies of the $\eta$-nucleus interaction near threshold, as a final–state interaction in a production reaction, can be used to determine the $\eta$-nucleus scattering length. In principle, this would permit conclusions to be drawn on the existence of such $\eta$-nucleus bound states. In order to disentangle the real and imaginary parts of the scattering length, reliable data very close to the production threshold is required [12]. The argument can be made more quantitative by looking directly at the expression for the expected energy dependence in the scattering–length approximation. If there is a near–by singularity (corresponding to a quasi–bound state) in the $\eta^3$He system, the effect of the $\eta$–nucleus final state interaction on the energy dependence of the production reaction is given by

$$\frac{1}{1+2\mathrm{Im}(a)\,k+|a|^2k^2}\ , \tag{1}$$

where $k$ denotes the centre–of–mass momentum of the outgoing $\eta$. Thus, to extract the real and imaginary parts of the scattering length $a$, measurements in a regime where $2\mathrm{Im}(a)k \sim |a|^2k^2$ are necessary. If we assume that $\mathrm{Im}(a) \sim 1$ fm and $\mathrm{Re}(a) \sim 4$ fm (this pair of values is in accordance with the existing data base) then the above formula would demand a measurement down to below 1 MeV of excess energy.

In Ref. [12] it was demonstrated that the energy dependence of currently existing World data set for $pd \to {}^3\mathrm{He}\,\eta$ shown in Fig. 1 seem to be consistent with a quite small imaginary part of the ${}^3\mathrm{He}\,\eta$ scattering length – this imaginary part might be significantly smaller than three times that of $\eta N$ scattering. Note, in Ref. [14] it was argued that this could possibly be understood as a consequence of the Pauli principle. In Ref. [7] it was stressed that a necessary condition for the existence of a $\eta^3$He bound state is that $|Re(a)| > Im(a)$. All these arguments clearly call for a high quality measurement of the reaction $pd \to {}^3\mathrm{He}\,\eta$ close to the production threshold. The existing discrepancies between the data available before the recent ANKE measurements are also reflected in Fig.1. In an attempt to clarify this situation, the COSY–11 collaboration studied this reaction at five different excess energies, $Q = 5.1$, 10.8, 15.2, 20.0, and 40.6 MeV [21]. These energies have been chosen to fill the gap that existed between $Q = 7$ MeV and $Q = 49$ MeV. In the region of excess energies studied these data confirm the quick levelling off of the total cross sections, as predicted by model calculations [22, 12].

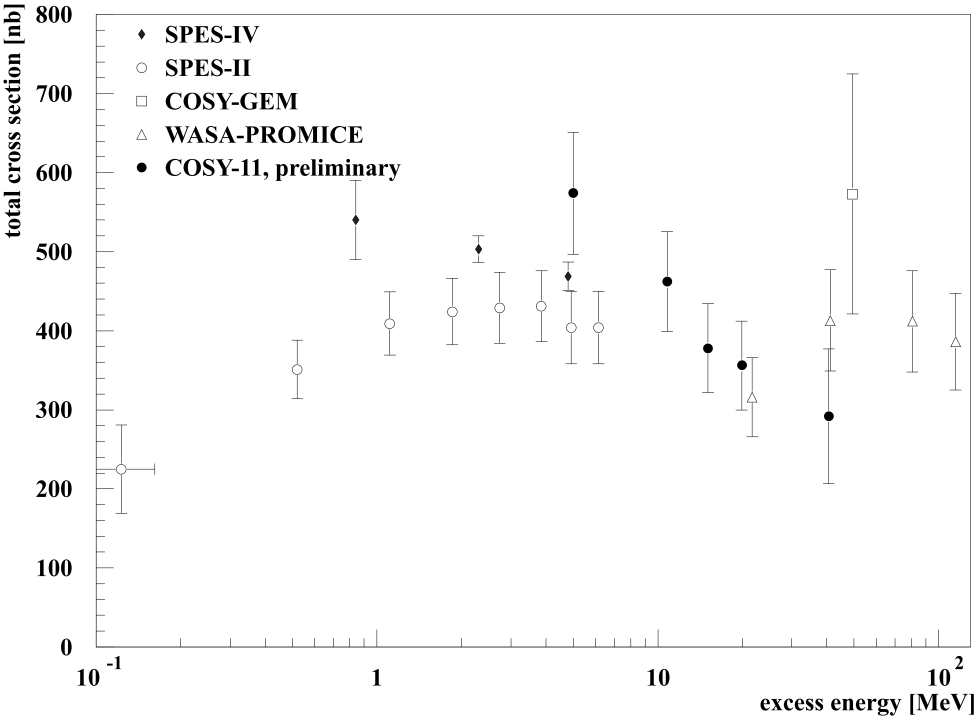


Figure 1: Energy dependence of the total cross section for the $pd \to {}^3\mathrm{He}\,\eta$ reaction. The data are from Refs. [15, 16, 17, 18, 19, 20, 21].

Here the energy dependence is assumed to be dominated by a strong ${}^3\mathrm{He}\,\eta$ final state interaction.

Since the existing data were still not sufficient to extract scattering length information with the required precision, new data with high statistics have been taken at the ANKE spectrometer with unpolarized beam and target [13]. Although still under evaluation, preliminary data on the excitation function confirm the strong variation of the total cross section very close to threshold, which differs markedly from pure phase space expectations. In Fig. 2 the preliminary ANKE data obtained at low excess energies are presented. Due to the high quality of the measurements, more precise information on the scattering length should be available in the near future.

However, the additional possibilities offered by the COSY polarized deuteron beam will allow us to investigate the underlying mechanism using a different approach. As discussed above, the $pd \to {}^3\mathrm{He}\,\eta$ reaction near threshold shows a very striking energy dependence [15, 17]. Despite the angular distribution remaining essentially isotropic, the square of the amplitude decreases by a factor of three over a few MeV in excess energy. The general feeling

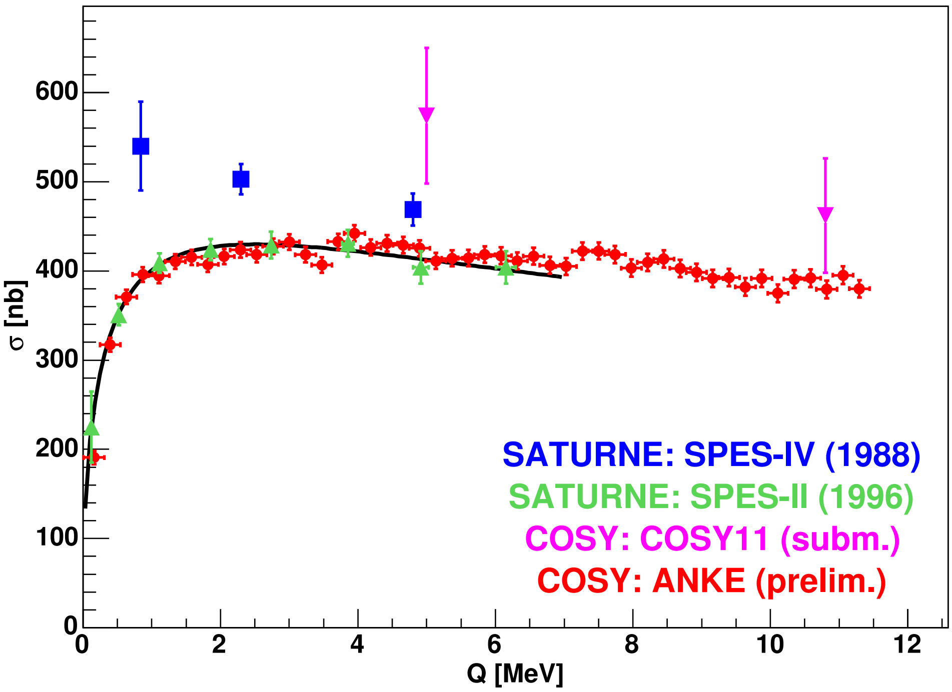


Figure 2: Preliminary data on the excitation function for the $dp \to {}^3\mathrm{He}\,\eta$ reaction, obtained at ANKE and arbitrarily scaled to the SPES-II data. The solid line presents a fit to the SPES-II data using the ${}^3\mathrm{He}\,\eta$ description from Fäldt and Wilkin [22, 12].

is that this is due to a very strong final state interaction between the $\eta$ and the ${}^3$He, which suggests that this system has a nearby pole in the complex momentum plane.

If the FSI interpretation is correct, the enhancement should depend only weakly upon the characteristics of the entrance channel and it is very important to verify this. Data on $\gamma\,{}^3\mathrm{He} \to \eta\,{}^3\mathrm{He}$ from Mainz [9] seem to show an even stronger energy dependence but these data are not as precise as the Saclay $pd \to {}^3\mathrm{He}\,\eta$ results and cannot be used to constrain the pole position.

Now close to threshold there are two independent $\eta$ $s$–wave $\vec{d}p \to {}^3\mathrm{He}\,\eta$ amplitudes. These can be thought of as spin-$\frac{3}{2}$ or spin-$\frac{1}{2}$ combinations of the $dp$ spins coupled with $L_{dp} = 1$ to give the overall $J = \frac{1}{2}^-$ state. An alternative decomposition was given by Germond & Wilkin [27] and used by Kerboul *et al.* [28] to describe the analogous $\pi^0$ production amplitudes in collinear kinematics:

$$f = \bar{u}_\tau \hat{p}_p \cdot (A\,\vec{\varepsilon}_d + iB\,\vec{\varepsilon}_d \times \vec{\sigma})\; u_p\,. \qquad (2)$$

The moduli-squared of the two amplitudes $A$ and $B$ can be separated by measurements of the differential cross sections and spherical tensor analyzing power $T_{20}$:

$$\frac{\mathrm{d}\sigma}{\mathrm{d}\Omega} = \frac{1}{3}\frac{p_\eta}{p_p}\left[|A|^2 + 2|B|^2\right] , \tag{3}$$

$$T_{20} = \sqrt{2}\left[\frac{|B|^2 - |A|^2}{|A|^2 + 2|B|^2}\right] . \tag{4}$$

Other analyzing powers, such as $T_{22}$ and $iT_{11}$ require higher $\eta$ partial waves and are expected to remain small close to threshold.

Now the pioneering experiment of the SPES-IV group [15] showed $T_{20}$ to be small (Fig. 3), so that both $|A|^2$ and $|B|^2$ are significant. However, the data were clearly insufficient to determine the energy dependence of the $A$ and $B$ amplitudes separately. This could also not be checked in the SPES-II experiment [17] because in this case a proton beam was used.

Therefore, we propose to extend our experimental programme to include the measurements of the energy variation of $|A|^2$ and $|B|^2$ near threshold in the $\vec{d}p \to {}^3\mathrm{He}\,\eta$ reaction to see whether the striking $\eta\,{}^3\mathrm{He}$ FSI effect is the same for two different entrance channels. The results should have a significant impact on the ongoing discussions of the possible existence of $\eta$–mesic nuclei. These planned measurements are in line with the proposed studies outlined in the ANKE spin document [29].

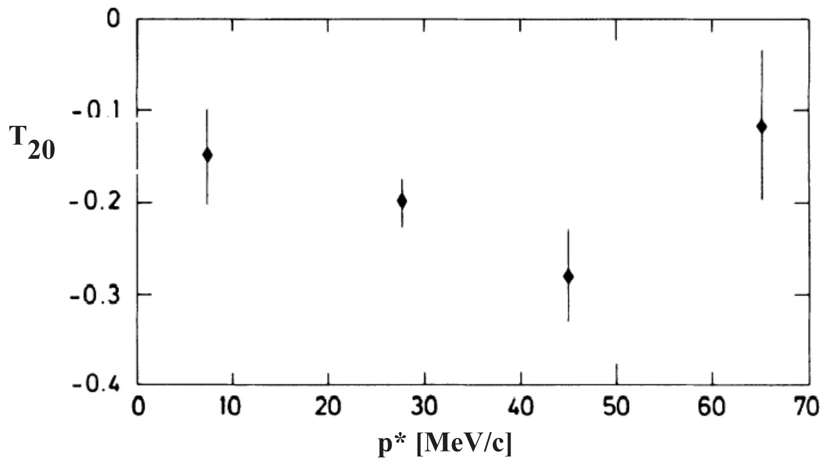


Figure 3: Deuteron tensor analyzing power $T_{20}$ for the $dp \to {}^3\mathrm{He}\,\eta$ reaction as a function of the $\eta$ cm momentum $p^*$. The figure was taken from [15].

## 2 The reaction $dp \to {}^3\mathrm{He}\,\eta$ at ANKE

Monte-Carlo simulations clearly show that the ANKE installation in combination with a deuteron beam is well suited for the study of the $dp \to {}^3\mathrm{He}\,\eta$ reaction from threshold up to higher excess energies. Fig. 4 shows Monte–Carlo generated tracks for this reaction channel at an excess energy of $Q = 20\,\mathrm{MeV}$. The outgoing ${}^3\mathrm{He}$–nuclei can be registered in the forward detection system while the four–momentum components of the produced $\eta$-mesons can be reconstructed using the missing mass technique. The main advantage of the ANKE facility is the large acceptance for this reaction channel, *i.e.* $\sim 100\%$, for excess energies ranging from threshold up to $Q \sim 20\,\mathrm{MeV}$. Important for

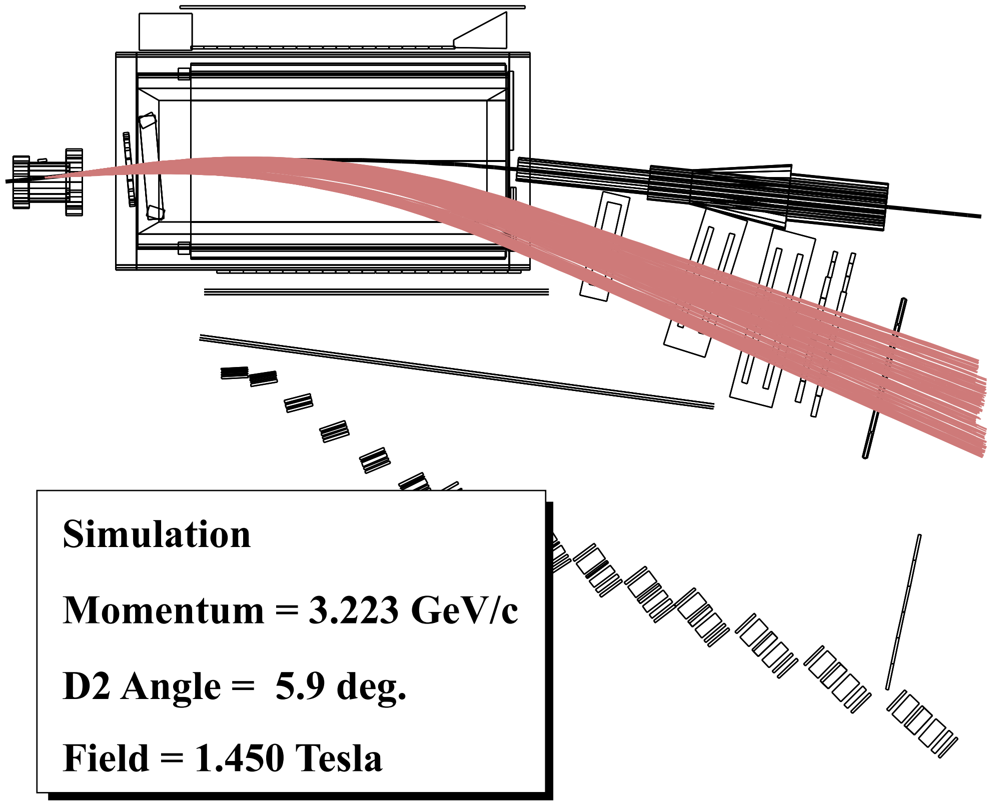


Figure 4: Sketch of the ANKE installation with Monte-Carlo simulated tracks from the $dp \to {}^3\mathrm{He}\,\eta$ reaction at an excess energy of $Q = 20\,\mathrm{MeV}$. Note that for excess energies up to 20 MeV the geometrical acceptance amounts to 100%.

the interpretation of the obtained data is a reasonable geometrical acceptance of the detection system for the whole range of polar scattering angles

$\vartheta$ in the centre–of–mass system. In Fig. 5 a sample of such acceptances is presented for excess energies of $Q = 20$, 40, and 60 MeV. At excess energies below 20 MeV the acceptance amounts to $\epsilon \sim$100% and no corrections have to be considered, and this reduces systematic uncertainties. Even at higher excess energies, the angular acceptance stays rather good and presents no gaps. It should also be noted that the ANKE installation quite generally provides large acceptances near $\cos\vartheta = \pm 1$.

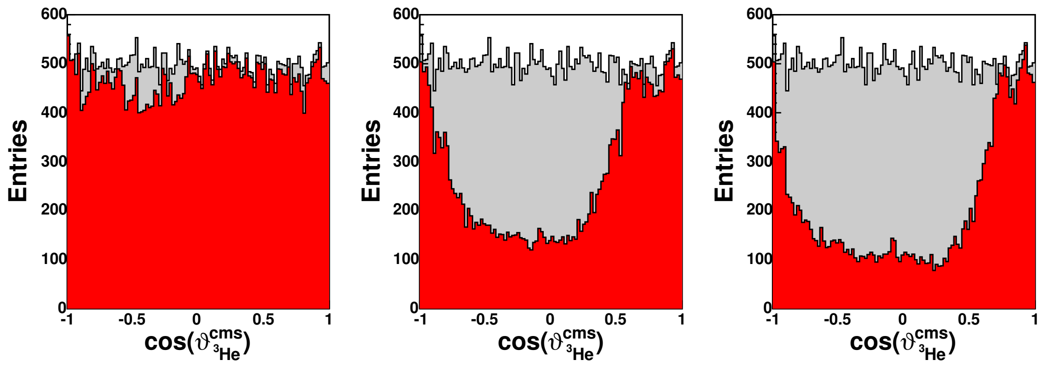


Figure 5: Geometrical acceptance of the ANKE spectrometer for the $dp \to {}^3\mathrm{He}\,\eta$ reaction at excess energies of $Q = 20$, 40, and 60 MeV.

The identification of emitted $^3$He-nuclei can easily be performed using the energy–loss information provided by the scintillation walls of the forward detection system. Therefore, this information can be used both for trigger purposes and event selection in the off–line data analysis. The produced $\eta$-mesons will be identified using the missing-mass technique.

The identification of different reaction channels is demonstrated by our recent unpolarized $dp \to {}^3\mathrm{He}\,\eta$ measurements shown in Fig. 6. This presents the reconstructed transverse *versus* longitudinal momentum of identified $^3$He nuclei. At large momenta ($|p| \sim 0.5$ GeV/c) a clear signal originating from single $\pi^0$ meson production is obvious. Due to the two–body kinematics, the events are distributed on a momentum ellipse, indicated by the outer solid line. The second ellipse ($|p| \sim 0.45$ GeV/c) indicates the maximum momenta for $^3$He nuclei originating from the two–pion production channels. Finally, the inner solid line represents the momentum ellipse of $^3$He nuclei from the $\eta$ meson production at $Q = 10$ MeV. As expected from the kinematics, the detected $^3$He nuclei are distributed well along this curve. Since the geometrical acceptance for this channel is close to 100% at this excess energy, contributions from higher partial waves already become visible within this figure.

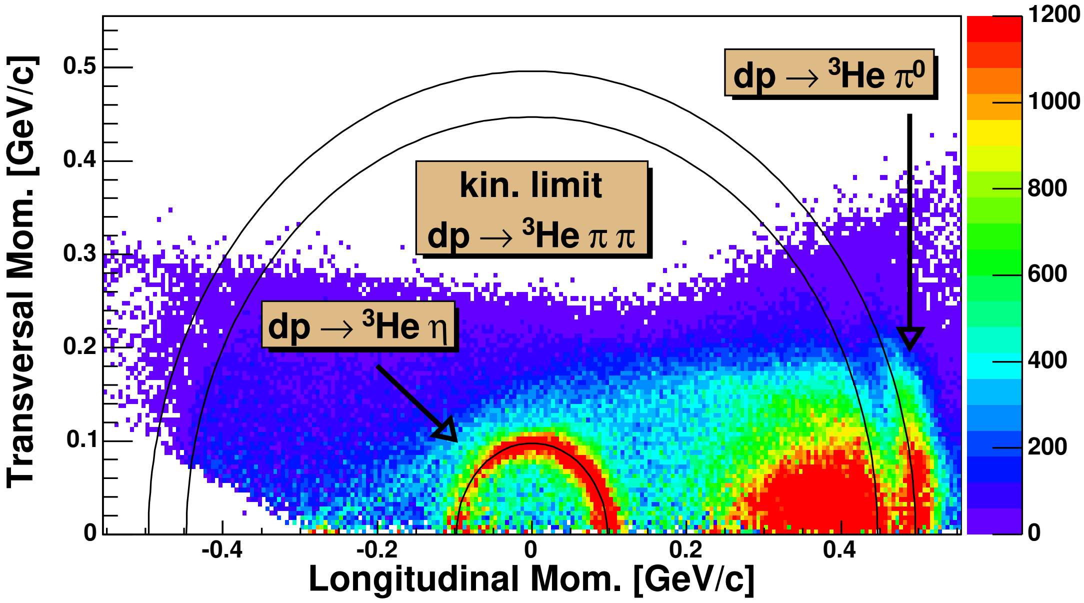


Figure 6: Identification of different meson reactions *via* a two–dimensional momentum plot. The solid lines indicate the expected momenta for the detected $^3$He nuclei resulting from single–meson production and, for double–pion production, the maximum momenta allowed by kinematics.

To extract quantitative information on total and differential cross sections, the missing–mass technique was applied to identify events from the $dp \to {}^3\mathrm{He}\,\eta$ reaction. During each cycle, the COSY beam was ramped from excess energies of $Q = -4.7\,\mathrm{MeV}$ up to $Q = +11.3\,\mathrm{MeV}$. In the analysis this energy range was divided into excess energy bins of $\Delta E = 237\,\mathrm{keV}$. Due to the high quality of the COSY beam and the high statistics obtained during the experiment, it is possible to determine the absolute value of the excess energy with a precision of $\Delta Q = \pm 107\,\mathrm{keV}$. This accuracy is of the utmost importance for the interpretation of the obtained data in the very–near–vicinity of the production threshold.

In the left hand side of Fig. 7 an example of an extracted missing–mass distribution is represented by the solid red line for events at an excess energy of $Q = (10.35 \pm 0.35)\,\mathrm{MeV}$. Since the $\eta$–meson peak is close to the kinematical limit, a careful subtraction of background events, mainly originating from multi–pion production channels, is essential in order to extract high quality data on differential and total cross sections. In the right hand side of Fig. 7 the corresponding missing–mass distributions are shown for $Q = -4.7\,\mathrm{MeV}$

(green curve) and $Q = -0.5\,\mathrm{MeV}$ (red curve). Here both data sets have been analyzed assuming an excess energy of $Q = -4.7\,\mathrm{MeV}$. In this way the kinematical limits of both distributions end at the same energies, which allows us to compare directly the shapes of these distributions. Subtracting both luminosity–corrected curves from each other results in the blue shaded histogram, which is compatible with zero. This shows that the energy dependence of the apparent background reactions can be neglected over the region of excess energies studied. In view of this, the sub–threshold data obtained during the COSY ramp can be used for the background description and subtraction at positive excess energies. This situation is shown in the left hand side of Fig. 7 by the green curve (background description) and the blue shaded histogram (residual $\eta$ meson signal). The high accuracy of this method is evident from the very good agreement of the measured background at lower missing masses with the one reconstructed using sub–threshold data.

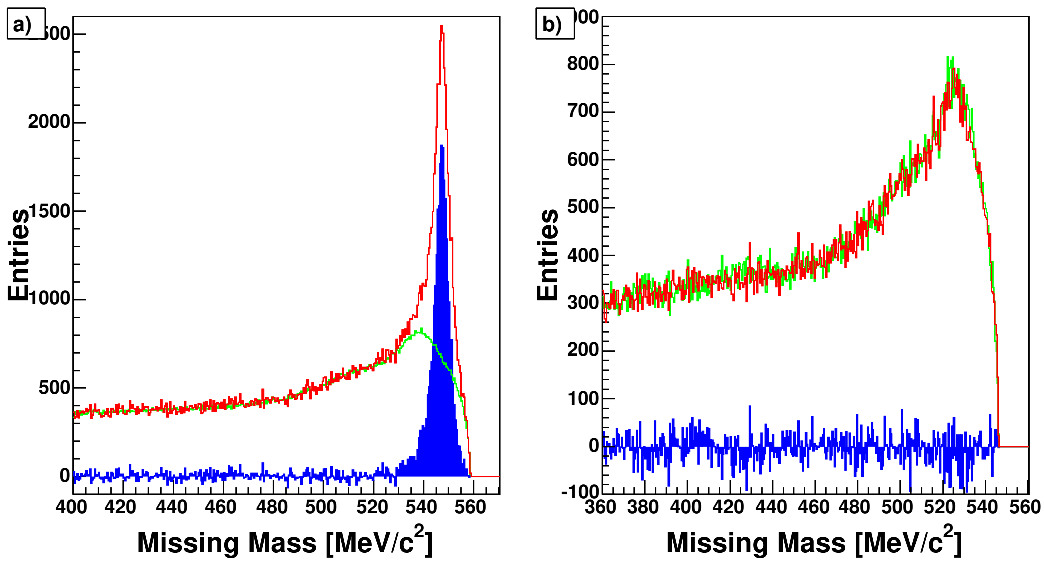


Figure 7: Description of the background in a missing–mass plot using the sub–threshold data.

The method has also been applied to extract differential cross sections. In Fig. 8 the missing mass distributions for different centre–of–mass angular bins are shown by the red curves. The background descriptions obtained at negative excess energies for the corresponding angular bins are indicated by the solid green lines and demonstrate once again the high accuracy of this method. Angular distributions can therefore be determined for each of the chosen excess energy bins. This method works well even at low excess energies, as can be seen from Fig. 9, which illustrates the $^3$He momentum distribution for an excess energy interval of $Q = (2.5 \pm 0.4)$ MeV [1].

The integrated luminosity will be determined for each energy bin by a simultaneous measurement of the *dp* elastic scattering. This reaction can be clearly identified through the detection of the scattered deuterons in the forward detector. Reliable reference data are available in our region of beam momenta and momentum transfers [25]. The relatively weak energy dependence of the *dp* elastic cross section over the small range of interest is also very helpful. Detailed information on this topic can be found in the ANKE beam time request #125 [26].

Preliminary total cross section data, arbitrarily scaled to the SPES-II data, are presented in Fig. 2. From this figure it is clear that the ANKE results are in very good agreement with those obtained at SATURNE. Due to the very high accuracy of the new data, the fine energy binning, as well as the extended energy range, especially at low $Q$, it is expected that one should be able to gain scattering length information with higher accuracy.

[1] For demonstration purposes the events have been weighted by the inverse of the transverse momentum.

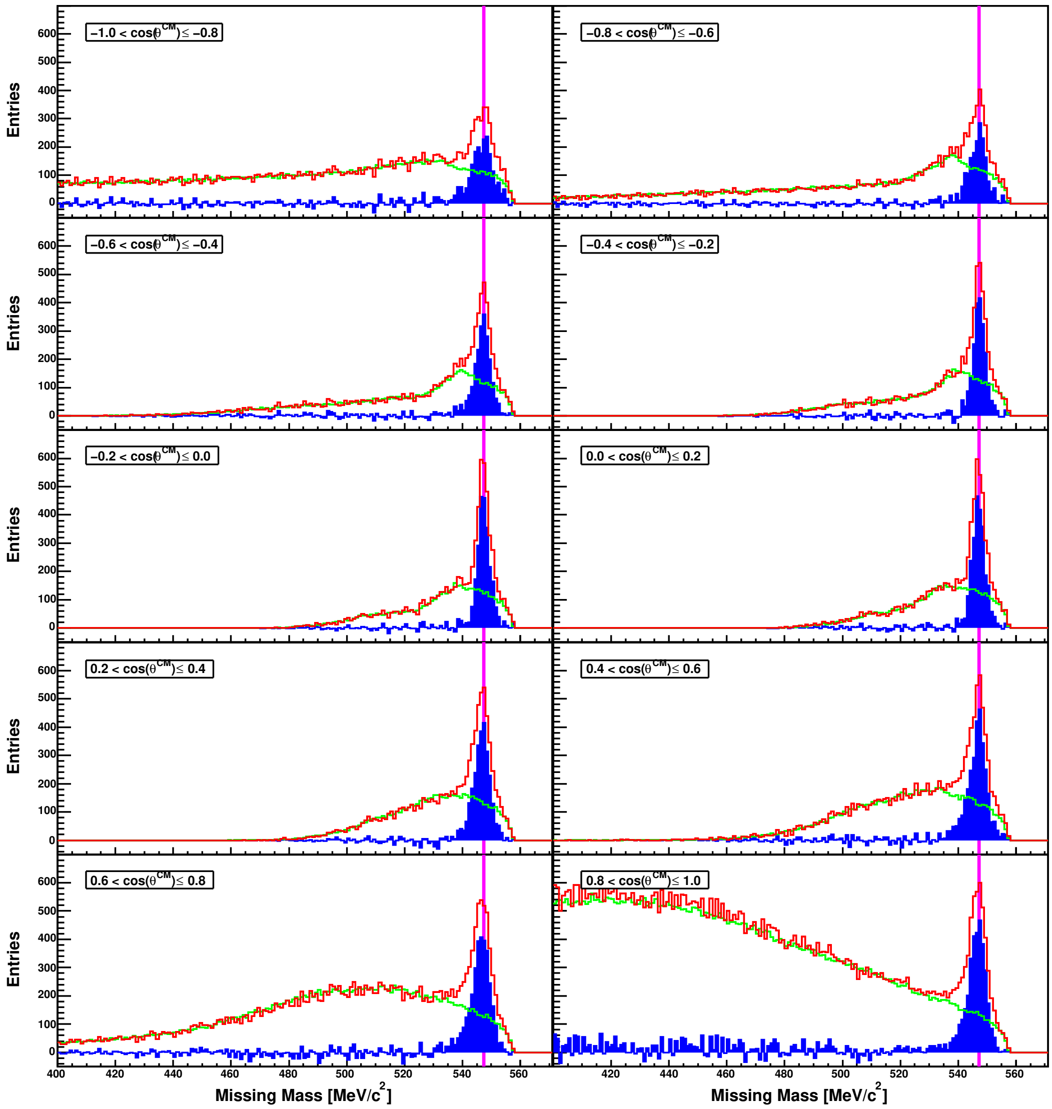


Figure 8: Determination of differential cross sections: For each $\cos\vartheta$ bin a separate missing plot will be analyzed using the background–subtraction method.

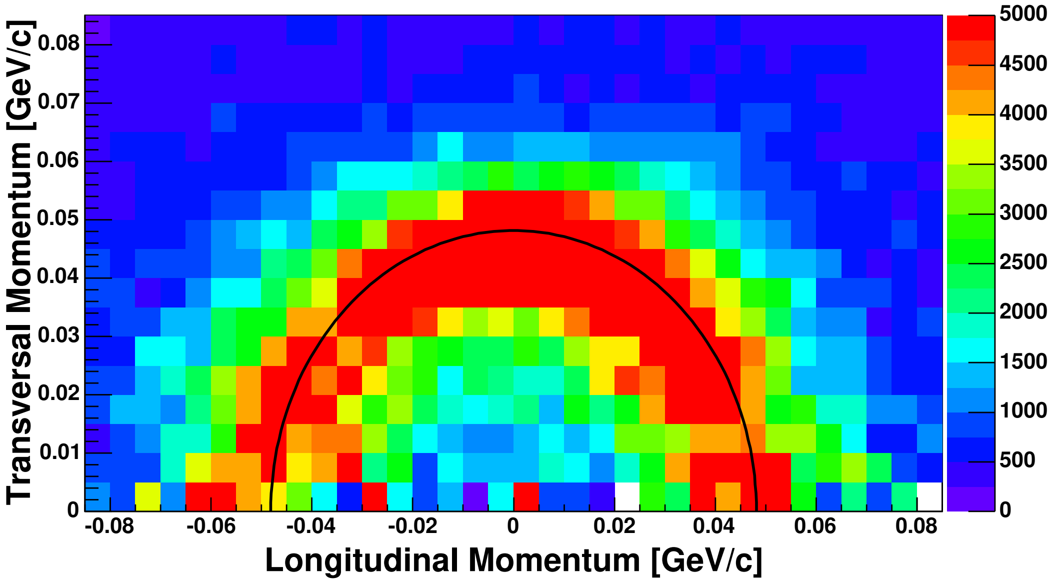


Figure 9: Transverse *versus* longitudinal momentum for $dp \to {}^3\mathrm{He}\,\eta$ events in an excess energy interval of $Q = (2.5 \pm 0.4)\,\mathrm{MeV}$.

# 3 Pilot measurement of the $\vec{d}p \to {}^3\mathrm{He}\,\eta$ reaction at ANKE

The feasibility of the proposed polarized measurements of the $\vec{d}p \to^3 \mathrm{He}\,\eta$ at ANKE is shown, to a large extent, by the success achieved with unpolarized deuteron beams. Before submitting a dedicated proposal, the reaction $\vec{d}p \to {}^3\mathrm{He}\,\eta$ has also been investigated parasitically in 2005 during an ANKE beam time on charge–exchange studies with polarized deuterons. Here one measurement was performed during $\sim 1.5$ days for eight different polarization modes at a COSY beam momentum of $p = 3.170\,\mathrm{GeV/c}$, corresponding to an excess energy of $Q = 7.4\,\mathrm{MeV}$ relative to the $\eta$ threshold. Although each polarization mode was investigated for only $\sim$4 h, signals of the $\eta$ meson production are clearly visible. In Fig. 10 the extraction of missing mass peaks for different angular bins is shown for a tensor polarized COSY beam[2]. In this preliminary study, the background was subtracted using information from the unpolarized measurements described before, though this necessitates some assumptions being made on the spin–dependence of the background.

For the proposed new measurements, it is planned to investigate the $\vec{d}p \to {}^3\mathrm{He}\,\eta$ reaction in a COSY ramp similar to the unpolarized measurements. Therefore, background information for each of the individual polarization modes will be available, which will allow us to reduce systematic errors.

The polarized differential cross section of a reaction can be written in terms of the unpolarized as [32]:

$$\frac{d\sigma^{\uparrow}}{d\Omega}(\vartheta,\phi) = \frac{d\sigma^{\circ}}{d\Omega}(\vartheta)\times$$
$$\left[1 + \frac{3}{2}P_z A_y(\vartheta)\cos\phi + \frac{1}{4}P_{zz}\left[A_{yy}(\vartheta)(1+\cos 2\phi) + A_{xx}(\vartheta)(1-\cos 2\phi)\right]\right], \tag{5}$$

where $A_y$, $A_{yy}$, and $A_{xx}$ are the vector and tensor analyzing powers for the reaction and $P_z$ and $P_{zz}$ are the vector and tensor polarizations of the beam. At threshold (or in the forward direction) the two Cartesian tensor analyzing powers are the same and $A_{yy} = A_{xx} = -\sqrt{2}T_{20}$, where $T_{20}$ is in the spherical representation.

The vector and tensor polarizations of the deuteron beam have been measured in ANKE at a beam energy of $T_d = 1.17\,\mathrm{GeV}$ by using a variety of nuclear reactions [30].

[2]Mode 4 has ideal values of $P_z$=0, $P_{zz}$=+1

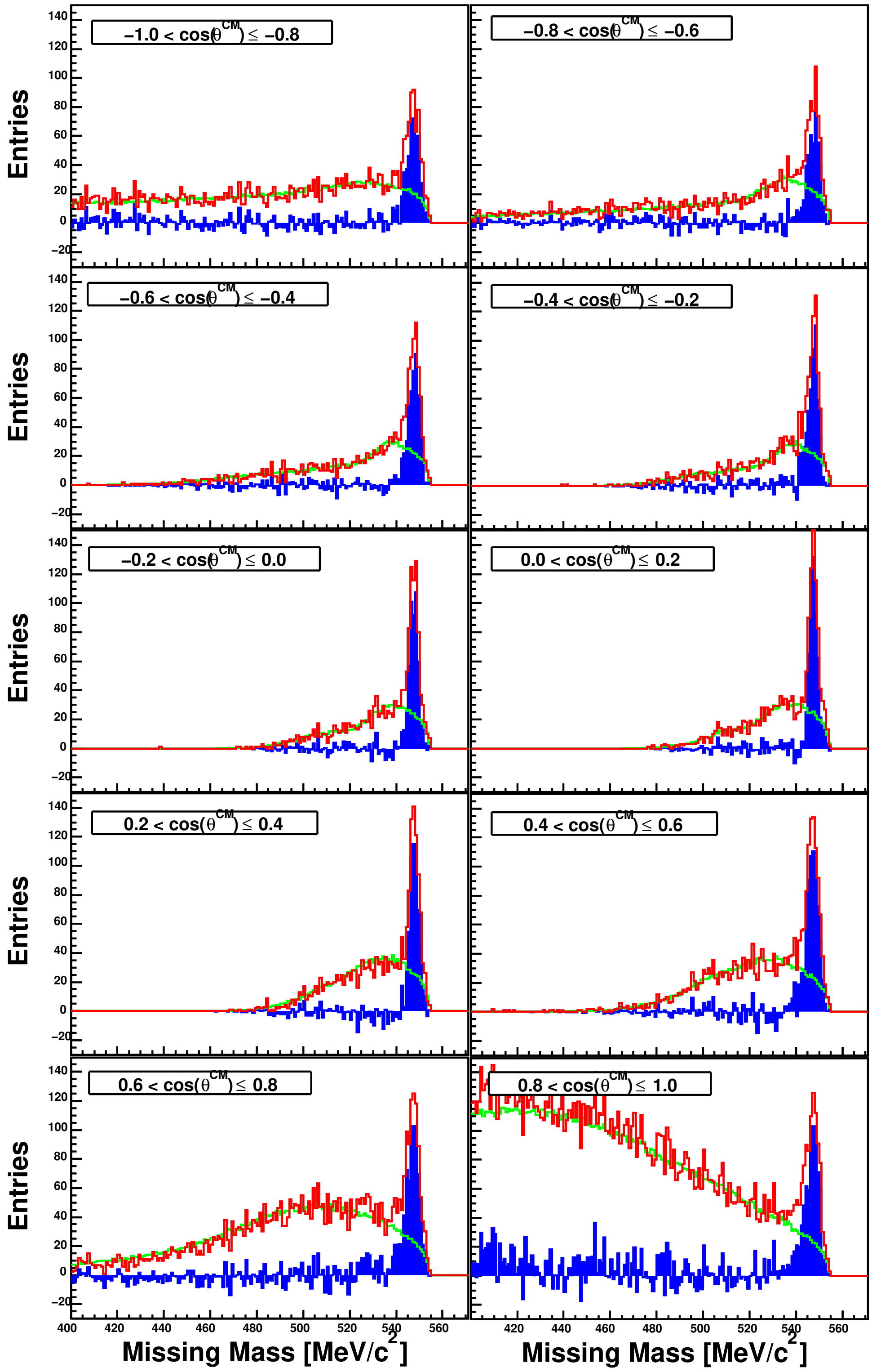


Figure 10: Determination of differential cross sections using a tensor polarized deuteron beam.

To establish the polarizations required for the $\eta$–production experiment, the *polarization export* technique will be used. This is standard for polarized proton beams [31]. The beam is first accelerated to say 1.2 GeV, the analyzing powers measured, and the beam then accelerated once again to the start of the ramp for the $\eta$–production. After the end of the ramp, the beam is decelerated to the calibration energy and the polarization remeasured to ensure that there is no polarization loss.

By way of illustration, if one uses a purely tensor polarized beam and compares the data with those obtained with an unpolarized beam, then at threshold:

$$T_{20} = \frac{2\sqrt{2}}{P_{zz}} \cdot \left( \frac{\frac{d\sigma^{\circ}}{d\Omega}(\vartheta) - \frac{d\sigma^{\uparrow}}{d\Omega}(\vartheta)}{\frac{d\sigma^{\circ}}{d\Omega}(\vartheta)} \right) \tag{6}$$

Together with Eq. (3) this allows us to obtain directly the squared amplitudes $|A|^2$ and $|B|^2$:

$$\begin{aligned} |A|^2 &= \frac{p_p}{p_\eta}(1 - \sqrt{2}T_{20})\frac{d\sigma}{d\Omega} \\ |B|^2 &= \frac{p_p}{p_\eta}(1 + \frac{1}{\sqrt{2}}T_{20})\frac{d\sigma}{d\Omega} \,. \end{aligned} \tag{7}$$

Now there is some evidence of higher partial waves even for $Q \sim 10$ MeV from our preliminary unpolarized angular distributions, which show a slightly non–isotropic behaviour. As a consequence, we can expect to extract values of $A_y$, $A_{xx}$ and $A_{yy}$ from the study of the $\phi$–dependence shown by Eq. (5). Preliminary results from our parasitic polarized measurements will be shown during the oral presentation.

# 4 Beam time request

In order to determine the energy dependence of the squared amplitudes $|A|^2$ and $|B|^2$ we propose to investigate the $\vec{d}p \to {}^3\mathrm{He}\,\eta$ reaction close to threshold using a ramped COSY beam, as has been previously done for the unpolarized measurements. Excess energies between $Q = -5\,\mathrm{MeV}$ and $Q = +11\,\mathrm{MeV}$ will be investigated. In principle, to obtain the values of $T_{20}$ it is sufficient to study $\eta$ meson production reaction with just two different polarization modes (*i.e.* unpolarized and tensor polarized beam). However, in order to minimize systematic errors and also extract values of (or limits on) $A_y$, it is appropriate to investigate this reaction with the four source modes presented in Table 1:

| **Mode** | $\mathbf{P_z}$ | $\mathbf{P_{zz}}$ | **Intensity** $I_0$ |
|---|---|---|---|
| 0 | 0 | 0 | 1 |
| 5 | 0 | $-2$ | 2/3 |
| 6 | $-1$ | $+1$ | 2/3 |
| 7 | $+1$ | $+1$ | 2/3 |

Table 1: Modes of the polarized deuteron ion source. Shown are the ideal values of the vector ($P_z$) and tensor ($P_{zz}$) polarizations and $I_0$ denotes the relative numbers of deuterons provided by the source.

To determine the different polarization modes $P_z$ and $P_{zz}$ for each COSY cycle, the *polarization export* will be used with each cycle starting and finishing at a fixed beam momentum of p = 2.435 GeV/c, corresponding to a beam energy of $T_d = 1.2$ GeV (see Fig. 11). For details see [29].

In total we ask for **two weeks** of beam time, including two days for beam preparation and trigger adjustment. Assuming similar luminosities as obtained for the previous unpolarized $dp \to {}^3\mathrm{He}\,\eta$ measurements, we expect for each excess energy bin of $\Delta Q = 1\,\mathrm{MeV}$ a total of **10,000 events**. Dividing the extracted angular distributions into angular bins of $\Delta\cos(\vartheta) = 0.2$, statistical uncertainties of 6% are expected for the differential cross sections. This number includes already the effect of background subtraction, which has been studied carefully using the unpolarized data.

In addition to the $\eta$–production data, we will also obtain results in parallel on elastic $\vec{d}p$ scattering, quasi–free $\vec{n}p \to d\pi^0$, and $\vec{d}p \to (pp)n$ at this threshold. This has already been achieved with ANKE at 1.2 GeV [30].

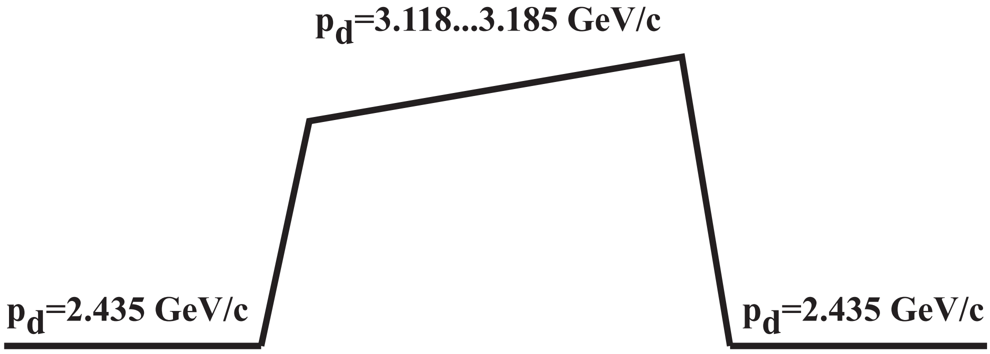


Figure 11: Investigation of the $\vec{d}p \to {}^3\mathrm{He}\,\eta$ reaction using a global jump in combination with a continuous ramp.

# 5 Future plans

With the measurements proposed here it will be possible to investigate the energy dependence of the amplitudes–squared $|A|^2$ and $|B|^2$, which can be directly compared with the average obtained for unpolarized data. In the FSI scenario, the same threshold enhancement should be seen for both amplitudes. However, the relative phase of $A$ and $B$ is not accessible in such an experiment. To gain information on this, a double polarization experiment is necessary. The reaction $\vec{d}\vec{p} \to {}^3\mathrm{He}\,\eta$ can be performed at ANKE using the polarized target and the storage cell and this will lead to a value of the $C_{yy}$ coefficient, for which

$$C_{yy} = -\frac{2Re(A^*B)}{|A|^2 + 2|B|^2}\,. \tag{8}$$

This measures the interference between those two amplitudes and is sensitive to differences between the two final state interactions. $C_{yy}$ will, of course, also be influenced by the different initial state interactions in the two cases, but these will be slowly varying over the few MeV over which the FSI is significant.

The amplitudes $|A|^2$ and $|B|^2$, as well as their relative phase, could also be studied by investigating the reaction $\vec{d}\vec{d} \to {}^3\mathrm{H}\,\eta + p_{\mathrm{spec}}$ with spectator proton, but we have currently no plans yet to propose such a study.

# References


[1] Q. Haider and L.C. Liu, Phys. Lett. B **172**, 257 (1986); **174**, 465 (E) (1986).

[2] R.S. Bhalerao and L.C. Liu, Phys. Rev. Lett. **54**, 865 (1985).

[3] T. Ueda, Phys. Rev. Lett. **66**, 297 (1991); N.V. Shevchenko *et al.*, Eur. Phys. J. A **9**, 143 (2000); S. Wycech and A.M. Green, Phys. Rev. **C 64**, 045206 (2001).

[4] A. Fix and H. Arenhövel, Eur. Phys. J. A **9**, 119 (2000); H. Garcilazo and M.T. Peña, Phys. Rev. **C 63**, 021001 (2001).

[5] S. Wycech, A.M. Green, and J.A. Niskanen, Phys. Rev. C **52**, 544 (1995).

[6] N. Willis *et al.*, Phys. Lett. B **406**, 14 (1997).

[7] Q. Haider and L.C. Liu, Phys. Rev. C **66**, 045208 (2002).

[8] C. Garcia-Recio, J. Nieves, T. Inoue and E. Oset, Phys. Lett. B **550** (2002) 47.

[9] M. Pfeiffer *et al.*, Phys. Rev. Lett. **92**, 252001 (2004).

[10] C. Hanhart, Phys. Rev. Lett. **94**, 049101 (2005).

[11] R.G. Newton, *Scattering Theory of Waves and Particles* (Springer-Verlag, New York, 1982).

[12] A. Sibirtsev, J. Haidenbauer, C. Hanhart and J. A. Niskanen, Eur. Phys. J. A **22**, 495 (2004).

[13] A. Khoukaz, T. Mersmann et al., COSY-Proposal #137: *Investigation of the* $^3He\,\eta$ *final state in the reaction* $dp \to {}^3He\eta$ *at ANKE*, (2004).

[14] V. Baru, C. Hanhart, A. E. Kudryavtsev and U. G. Meissner, Phys. Lett. B **589**, 118 (2004).

[15] J. Berger *et al.*, Phys. Rev. Lett. **61**, 919 (1988).

[16] J. Banaigs *et al.*, Phys. Lett. B **45**, 394 (1973).

[17] B. Mayer *et al.*, Phys. Rev. C **53**, 2068 (1996).

[18] R. Bilger *et al.*, Phys. Rev. C **65**, 044608 (2002).

[19] M. Betigeri *et al.*, Phys. Lett. B **472**, 267 (2000).

[20] T. Kirchner, PhD Thesis, Institut de Physique Nucléaire, Orsay (1993).

[21] H.-H. Adam, PhD Thesis (in preparation), Institut für Kernphysik, Universität Münster, Germany (2006); submitted to Phys. Rev. C.

[22] C. Wilkin, Phys. Rev. C. **47**, R938 (1993).

[23] M. Stenmark, Phys. Rev. C **67**, 034906 (2003).

[24] A. Kacharava et al., COSY-Proposal #125: *The polarized charge exchange reaction d(pol.)+p* $\rightarrow$ *(pp)*$^1S_0$*+n*, (2003).

[25] N. Katayama *et al.*, Nucl. Phys. A **438**, 685 (1985).

[26] A. Kacharava et al., COSY Beam Request for the Proposal #125: *First measurement of the Charge-Exchange np* $\rightarrow$ *pn Reaction with Polarized Deuteron Beam at ANKE*, (2004).

[27] J.-F. Germond & C. Wilkin, J. Phys. G **14**, 181 (1988).

[28] C. Kerboul *et al.*, Phys. Lett. B **181**, 28 (1986).

[29] A. Kacharava, F. Rathmann, C. Wilkin, COSY Proposal #152: *Spin Physics from COSY to FAIR*, (2005).

[30] D. Chiladze *et al.*, submitted to Phys. Rev. ST–AB.

[31] S. Yaschenko *et al.*, Phys. Rev. Lett. **94**, 072304 (2005).

[32] G.C. Ohlsen, Rep. Prog. Phys. **35**, 717 (1972).